LA-UR-06-0512

Title: RESIDUAL STRESS MEASUREMENTS IN A THICK, DISSIMILAR ALUMINUM-ALLOY FRICTION STIR WELD

Author(s):
Michael B. Prime (ESA-WR)
Thomas Gnäupel-Herold (NIST, Maryland)
John A. Baumann (Boeing St. Louis)
Richard J. Lederich (Boeing St. Louis)
David M. Bowden (Boeing St. Louis)
Robert J. Sebring (MST-7)

Details:
Acta Materialia
Volume 54 number 15
September 2006
pp. 4013-4021

Residual Stress Measurements in a Thick, Dissimilar Aluminum-Alloy Friction Stir Weld

Michael B. Prime[a,*], Thomas Gnäupel-Herold[b], John A. Baumann[c], Richard J. Lederich[c], David M. Bowden[c], Robert J. Sebring[a]

[a] Los Alamos National Laboratory, Los Alamos, New Mexico, USA 87545

[b] NIST Center for Neutron Research, Gaithersburg, MD 20899-8562

[c] The Boeing Company, St. Louis, MO 63166-0516

Abstract

25.4-mm thick plates of aluminum alloys 7050-T7451 and 2024-T351 were joined in a butt joint by Friction Stir Welding (FSW). A 54-mm long test specimen was removed from the parent plate, and cross-sectional maps of residual stresses were measured using neutron diffraction and the contour method. The stresses in the test specimen peaked at only about 32 MPa and had the conventional "M" profile with tensile stress peaks in the heat-affected zone outside the weld. The asymmetric stress distribution is discussed relative to the FSW process and the regions of highest thermal gradients. The general agreement between the two measurement techniques validated the ability of each technique to measure the low magnitude stresses, less than 0.05% of the elastic modulus. Subtle differences between the two were attributed to spatial variations in the unstressed lattice spacing (d_0) and also intergranular strains affecting the neutron results. The FSW stresses prior to relaxation from removal of the test specimen, were estimated to have been about 43 MPa, demonstrating the ability of FSW to produce low-stress welds in even fairly thick sections. To avoid the estimated 25% stress relaxation from removing the test specimen, the specimen would have had to be quite long because the St. Venant's characteristic distance in this case was more related to the transverse dimensions of the specimen than the plate thickness.

* Corresponding author, Tel: +1 505 667-1051, fax +1 505 665-6333, email: prime@lanl.gov

I. Introduction

Friction Stir Welding (FSW) is a revolutionary joining process which has seen remarkable growth in research, development and application in recent years. Conventional structural components for aircraft – beams for floors, spars, with tailored characteristics to meet durability and damage tolerance requirements, and so on – are normally built-up using discrete components of different alloys. To reduce the costs associated with conventional alignment and assembly steps of built-up structure, ever more assembled components are being converted to unitized structure via such processes as casting or machining from forged preforms or thick plate stock. Friction Stir Welding offers additional avenues to unitization of structural components. Lap and butt joining of thin sheet materials provides an alternative to conventional joining/fastening. Another pathway to structural components is the fabrication of "tailored blanks," using FSW to join shaped blocks of plate or forgings, from which unitized parts may be machined. Both of these approaches are in various stages of development and production.

FSW has sufficiently matured such that direct joining of 1-inch thick plates of 2XXX or 7XXX Aluminum Alloys (AA) is currently within the state of the art, creating starting stock with distributed property characteristics [1]. Static strengths in such joints typically exceed 80% of the parent strength of the weaker alloy. Investigations of durability characteristics are underway. A significant potential contributor to the durability behavior of FSW joints and surrounding material, however, will be the magnitude and distribution of residual stress imparted by the FSW process. Crack growth rates in test coupons of FSW in aluminum alloys have been observed to change in the region of friction stir welds. Detailed testing has shown that that the rate changes occur primarily from residual stresses, even at very modest magnitudes, rather than microstructural changes [2-6]. Therefore, knowledge of residual stresses is crucial if accurate property measurements are required. Furthermore, residual stresses in structures would be expected to differ from those in test coupons. Therefore, knowledge of residual stresses in structural components, not just test coupons, is also critical.

The measurements presented in this paper of internal residual stresses in a 25.4-mm thick FSW of dissimilar aluminum alloys provided measurement challenges beyond what has been previously reported in the literature. All previous reports of FSW residual stresses were for thicknesses of 10-mm or less and mostly for monolithic welds. Some surface and near-surface results have been reported using X-ray diffraction [7, 8] and hole-drilling [4, 9]. Through-thickness stresses were measured by hole-drilling in a 3-mm thick FSW in various aluminum alloys [10]. Using layer removal, X-ray measurements have been used to reconstruct internal stresses [5]. The vast majority of results for subsurface residual stresses have been reported from neutron diffraction and synchrotron X-ray diffraction measurements. Such measurements generally require an unstressed reference lattice spacing (d_0) in order to determine strains from measured lattice spacings [11]. Unfortunately, the FSW process often results in inhomogeneity and spatial variations of the unstressed lattice spacing, which must then be measured or otherwise addressed. The unstressed spacing in FSW specimens has been measured by sectioning a reference piece to obtain stress relief [12-14], which is tedious and arguably renders the neutron measurement destructive. In thin FSW specimens, the assumption of zero stresses in the direction of the plate normal has been used to overcome the reference issue [15-18], but this assumption becomes less sure as the sample thickness increases and some have reported measuring significant magnitudes for this stress component [14]. Sometimes, the varying reference spacing issue is not accounted for and leads to issues in interpreting the results [19]. For thin samples and when thickness-averaged stresses are acceptable, the *d* vs. $\sin^2\psi$ technique has been used with synchrotron X-ray diffraction to bypass the reference spacing issue [11]. The only significant exploitation of the non-destructive nature of diffraction measurements involved using synchrotron X-ray diffraction to measure the evolution of residual stresses during fatigue cycling [12]. Destructive measurements using incremental slitting (crack compliance) have provided particularly insightful measurements for examining the effect of residual stress on fatigue crack growth [2, 6, 8]. Only two works report results in dissimilar friction stir welds, and they were both under 4-mm thick [18, 20].

This study will compare contour method [21] measurements with neutron diffraction measurements. Each method has its inherent strengths and weaknesses which

complement each other in several key areas, thus enabling a thorough investigation of the stress state in this specimen. The contour method is destructive, but it is quite insensitive to inhomogeneities in the specimen as long as they do not significantly affect the elastic constants. The contour method has been demonstrated to be able to measure residual stresses in many applications, such as thick sections, that would be difficult or impossible for other methods. Examples include 107-mm thick aluminum alloy forgings [22], stresses from a ballistic penetration event in a 51-mm thick plate of HSLA-100 steel [23], laser-peening stresses in thick plates of a corrosion-resistant Ni-Cr-Mo alloy [24], and stresses in railroad rails [25].

The measurements in this study fulfill a secondary purpose of validating the contour method for low magnitude stresses. The contour method has been validated by comparing with neutron diffraction measurements in a TIG-welded steel plate [26] and a 316L stainless steel plate with an metal-arc weld bead [27] and by comparing with both synchrotron X-ray and neutron diffraction data in an aluminum weldment [28]. In those applications, the peak residual stress magnitudes were 0.35%, 0.17% and 0.25% of the elastic modulus, respectively. In this study, the stress magnitudes ended up being less than 0.05% of the elastic modulus, therefore testing the sensitivity of the method to low stresses.

II. Experiments

A. Specimen Preparation

25.4-mm thick plates of 7050-T7451 and 2024-T351 were procured from a commercial vender. The temper designations indicate that the plates were stress relieved by uniaxially stretching in the rolling direction to at least 1.5% plastic strain. The Edison Welding Institute (EWI) in Columbus, OH performed friction stir butt welding to produce a 305-mm × 457-mm plate from two 153-mm × 457-mm plates as shown in Figure 1. A one-pass single sided joint was formed at a rate of 50.8 mm per minute using a threaded-pin FSW tool. This particular weldment was fabricated by locating the 2024-T351 panel on the advancing side of the weld. X-ray radiography and metallographic cross sections verified that the joint was sound and free of voids and root surface

disbands. After welding the panel was aged at 121°C for 24 hours to stabilize the weld nugget. A significant portion of the panel was consumed by microstructure and mechanical property characterization. A 54-mm × 162-mm sample was extracted for residual stress determinations.

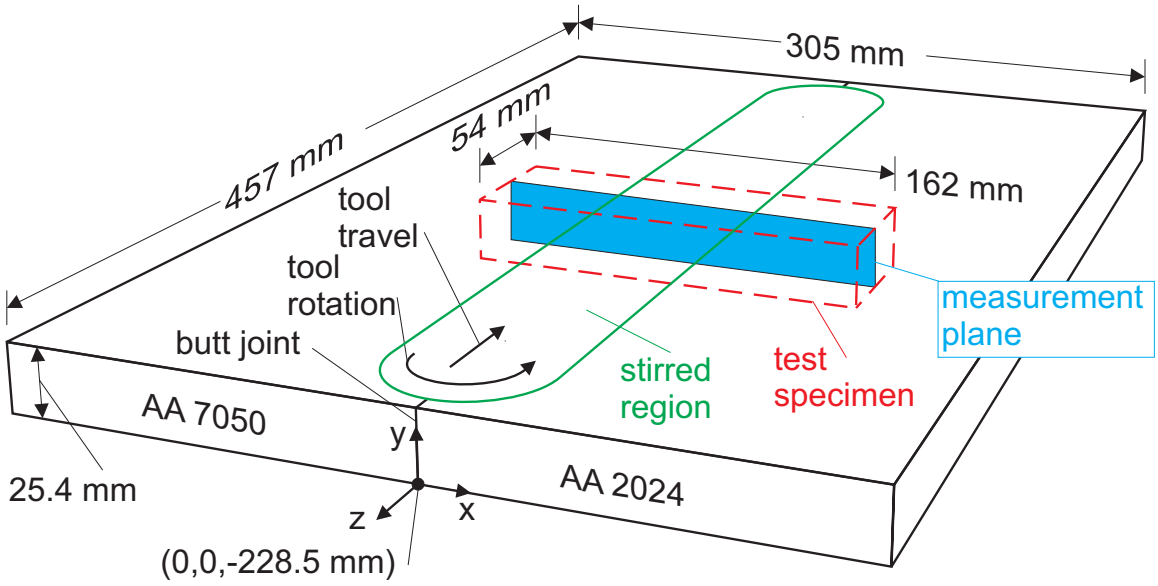

Figure 1. The parent weld plate showing dimensions and location of test specimen that was removed from the center.

B. Contour Measurements

The test specimen was cut in half on the measurement plane indicated in Figure 1 with a Mitsubishi FX-10K wire EDM machine using a 100-µm diameter brass wire. To minimize movement as stresses were relaxed during the cutting, the specimen was securely clamped to a 19-mm thick steel plate, which was in turn clamped in the EDM machine. The cut was made with the 25-mm specimen thickness in the direction of the wire axis. The part was submerged in temperature-controlled deionized water throughout the cutting process. To prevent any thermal stresses, the weld specimen and fixtures were allowed to come to thermal equilibrium in the water tank before clamping. "Skim cut" settings, which are normally used for better precision and a finer surface finish, were used because they also minimize any recast layer and cutting-induced stresses. The cut started on the 7050 side of the specimen, and it took 12 hours to complete the 162-mm long cut. Test cuts to check cutting flatness were later made in nearly stress-free regions of both aluminum alloys.

After cutting, the parts were unclamped from the fixture. The contours of the cut surfaces were measured using a Keyence LT-8105 confocal laser ranging probe with a spot 7 μm in diameter [26]. The nominal accuracy of the probe was ±0.2 μm. The surface was scanned by rastering the probe using orthogonal air-bearing translation stages. The motions of the laser scanner were confirmed to remain flat to sub-μm accuracy by measuring an optical flat. The specimen in this study was scanned using rows separated by 0.34-mm with data points within a row sampled every 0.1-mm. This resulted in about 153,000 points on each surface, which significantly exceeds the required density.

The stresses that were originally present on the plane of the cut were calculated numerically by elastically deforming the cut surface into the opposite shape of the contour that was measured on the same surface [21]. This was accomplished using a 3-D elastic finite element (FE) model. A mesh was constructed of one half of the part—the condition after it had been cut in two. The mesh used 18,900 bi-quadratic (20 node) hexahedral elements. The material behavior was taken at isotropic and linearly elastic.

A single value of elastic modulus was used for all regions in the model. Typical values for the elastic modulus of 2024 aluminum are 73.1 GPa in tension and 74.5 GPa in compression, and for 7050 aluminum 70.6 GPa in tension and 72.7 GPa in compression [29]. The average, 72.7 GPa, of these values was used. The range in these values of ±3% from the average is no greater than other error sources in the measurement; therefore, the effort to more precisely account for spatial variations in elastic modulus is not warranted. Poisson's ratio was taken as 0.33, which is the reported value for both 2024 and 7050.

For the FE stress calculation, the opposite of the measured surface contour was applied as displacement boundary conditions on the surface corresponding to the cut. The steps outlined here to process discrete surface contour data, i.e., the point clouds, are described in more detail elsewhere [26]. The point clouds from the two opposing surfaces created by the cut were aligned to each other, interpolated onto a common, regular grid and then averaged point by point. (Averaging the two contours is crucial to minimize several error sources [21]). Next, the data were fit to a surface using smoothing splines. The amount of smoothing was selected by minimizing the estimated uncertainty in the results. Finally, heights of the smoothed surface were evaluated at the coordinates of the nodes in the finite element model, the signs were reversed, and the results were written

into the FE input file as displacement boundary conditions in the normal direction. The transverse displacements on the cut surface were left unconstrained in the FE input file, which by default enforces the condition of zero shear stresses on the surface. Even if shear residual stresses were originally present, this procedure still obtains the correct result for the normal residual stresses [21].

C. Neutron Measurements

Prior to the contour measurements, the neutron diffraction measurements were done using the BT8 neutron diffractometer at the NIST Center for Neutron Research. As the technique is well-established and described elsewhere [30], only the specifics of this experiment are given.

A wavelength of 1.781 Å was chosen such that the (311) lattice plane used here was approximately at $2\theta = 92^{\circ}$. A $4\times4\times4$ mm^3 gauge volume in combination with a 4-mm depth (z-direction) oscillation was used to minimize fluctuations resulting both from grain size and from the mixing of the AA7050 and the AA2024 within the weld zone. The d-spacings of both alloys in the unstressed state are different which can cause fluctuations in the measured d-spacings in the weld zone if the gauge volume is located predominantly within a streak of 2024 or within 7050. In order to improve the grain average further the specimen was rocked within ±2º of the respective strain direction. The arrangement of the gauge volumes and their approximate size is shown in Figure 2.

Strains were measured along the three principal direction at the locations shown with a typical relative uncertainty of 5×10^{-5}. The option of sectioning the specimen after the measurement in order to obtain d_0-measurements exactly at the locations of the strain measurements was not available. Using small coupons cut off from the side of the specimen the measurement of the unstressed d-spacings showed large fluctuations of results between neighboring locations even within the base materials, see Figure 3, that lead to large uncertainties in the stresses.

As the location of these measurements was different from the location of the strain measurements, and because of the magnitude of the fluctuations, a different approach for unstressed lattice spacing was chosen in which the condition $\sigma_y=0$ was applied. This is true exactly at the surface only but the condition is fulfilled with good

accuracy also for thin plates. However, because of the specimen thickness of 25-mm the condition may not be fulfilled in the mid-plane to the same extent as close to the surface. Also, intergranular stresses, i.e. the stresses between grains may still affect the results. Nonetheless the benefit of applying this condition point wise – and thus correcting to some extent for d_0-variations – outweighs the disadvantage of using d_0-values from different parts of a specimen that is clearly very inhomogeneous.

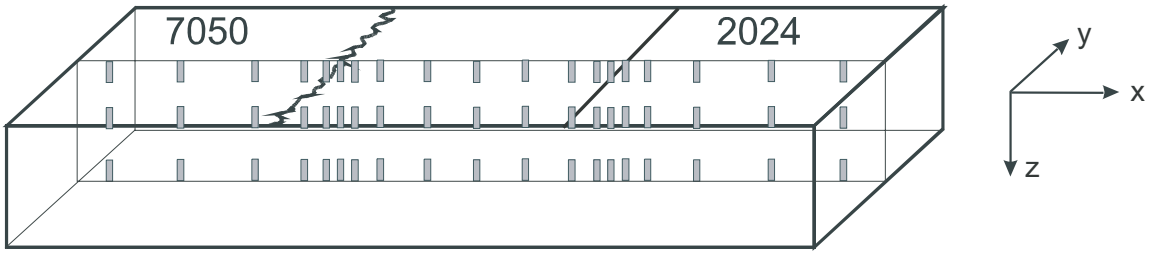

Figure 2. Location of gauge volumes for the neutron measurements. The boundaries of the weld zone are marked on the top surface.

For one direction a more detailed measure of d_0-variations could be obtained after sectioning of the specimen for the contour measurements (Fig. 3b). Using this method, the strain free direction ψ^* is determined from X-ray diffraction measurements of the two perpendicular stress components σ_x and σ_z [31]. The y-component is perpendicular to the free surface, and it is set to zero because of the shallow penetration of the X-rays (≈ 20 μm). The additional information obtained by X-ray diffraction is the considerable difference of d_0-values between top/bottom and the middle of the specimen. Figure 3 shows that the values of d_0 depend on both on location and the measurement direction. The specimen investigated here consists of two different alloy parts and a mixing zone, each of which expectedly with different d_0. Additionally, the alloy parts were exposed to thermal gradients during the welding which potentially contributed to the d_0 gradients in the alloy parts. Thus, for best accuracy in the stress determination, d_0 measurements would be required at every location and in every direction in which an actual diffraction strain measurement is performed.

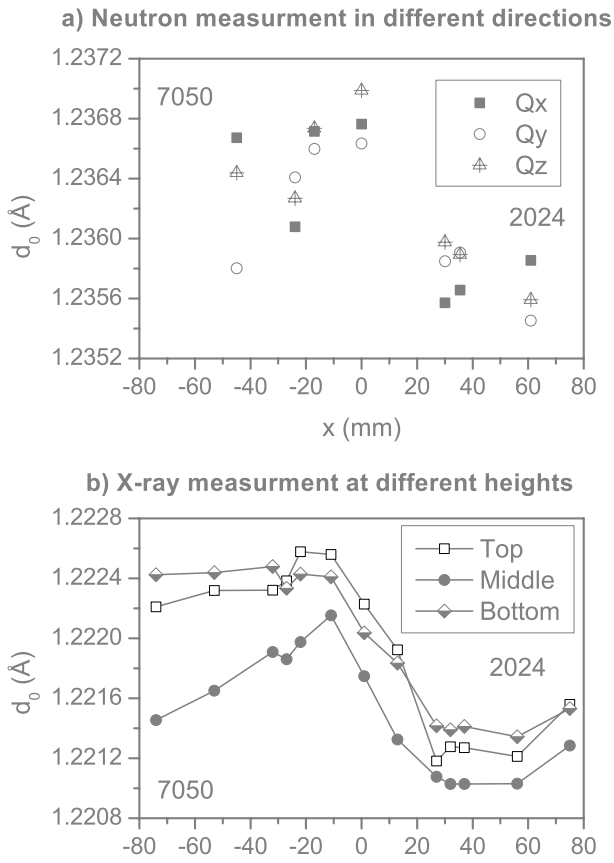

Figure 3. Results of (a) neutron diffraction d0-measurements and (b) X-ray measurements representing the average of d0 for the Qz and Qx directions. The strain uncertainty both for the neutron and the X-ray results is typically $< 2 \times 10^{-5}$. There is a constant offset between the values in (a) and in (b) because the neutron wavelength is known only with limited accuracy.

III. Results

Figure 4 shows the macrostructure of the weld on the same cross-section as the stress measurements. The overall structure is consistent with the observations in the literature for FSW in thinner plates, e.g., [3, 14, 32]. The stirred zone, i.e., the weld nugget or dynamically recrystallized zone, approximately coincides with the shape of the tool and contains fine, equiaxed grains. The onion ring structure in the nugget is evident. On both sides of the stir zone are Thermomechanically Affected Zones (TMAZ) which contain highly deformed grains from the stirring action. The TMAZ is more optically distinct on the advancing side and more diffuse on the retreating side. The heat-affected

zones extend out of the frame of the picture on both sides. Approximate boundaries between the regions will be overlaid on residual stress measurement results in order to aid interpretation.

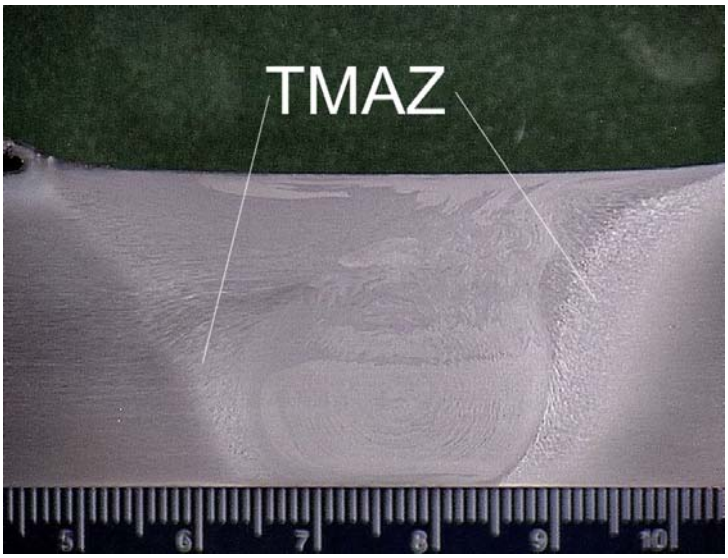

Figure 4. Metallographic cross-section of welded plate. The right side is the 2024 alloy and advancing side of the weld. The left side of the figure is the 7050 alloy. The scale is in centimeters. The approximate locations of the Thermo-Mechanically Affected Zones (TMAZ) are indicated.

Figure 5 shows the results of the laser scan of the cut surfaces. The contours roughly resemble a "W" shape with low spots on either side of the weld region. The peak-to-valley range of the contour is about 20 μm. The test cuts in low stress regions elsewhere in the part were flat to within less than 1 μm, indicating that the contour shape in Figure 5 is caused by stress relaxation and not by the EDM cutting.

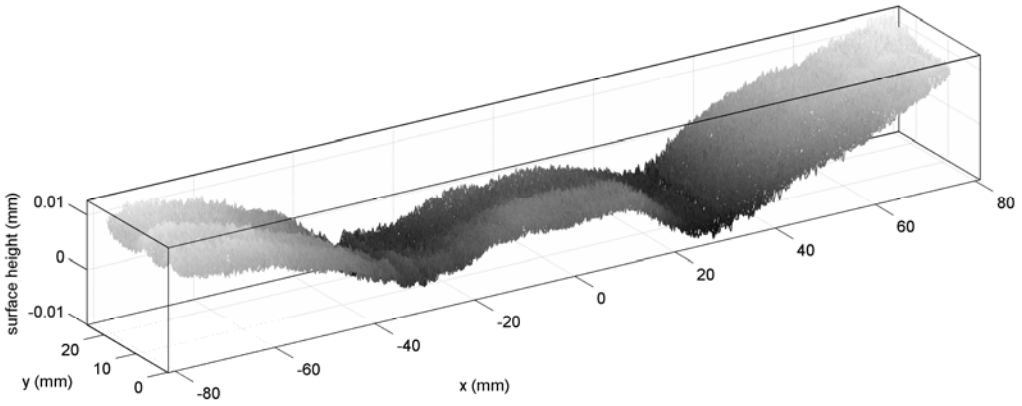

Figure 5. Surface contour caused by cutting the specimen in two and relaxing the residual stresses. Plotted is the average of the contours measured on the two opposing surfaces created by cutting.

Figure 6 shows the finite element model used to calculate the residual stresses from the measured surface contours.

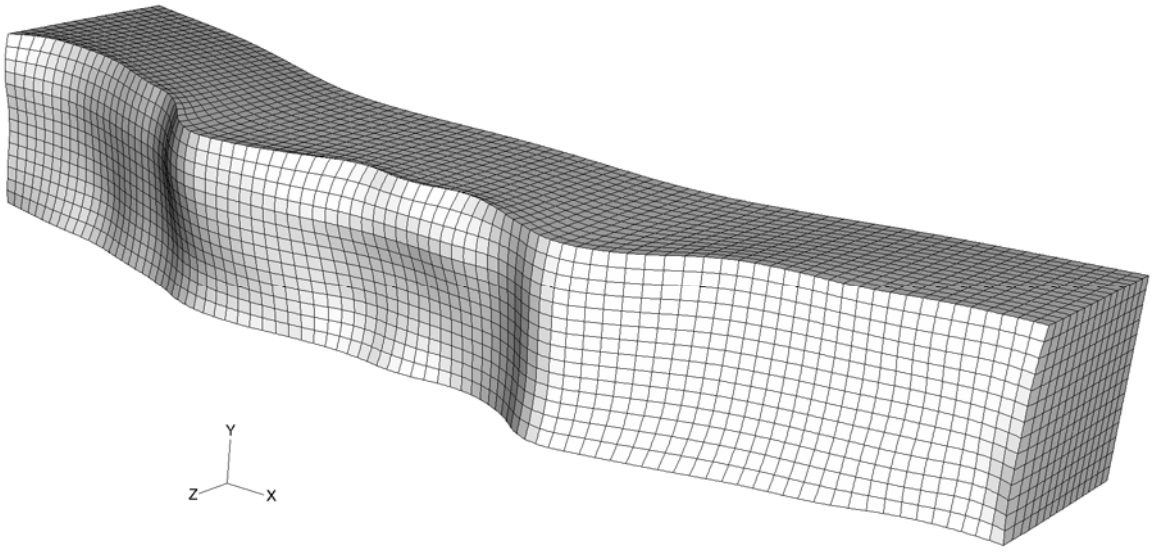

Figure 6. Elastic finite element of half of test specimen with cut surface deformed into opposite of measured surface contour. Displacements magnified by factor of 1000.

Figure 7 shows the contour-method results for the longitudinal stresses on the measurement plane shown in Figure 1. The stress magnitudes range from about -30 MPa to +32 MPa. These magnitudes are only about 0.044 % of the elastic modulus, which

could make measurement sensitivity an issue for many measurement methods. Nonetheless, the surface contour was significant enough to measure easily, making the results reasonably precise with an estimated uncertainty of about ±5 MPa.

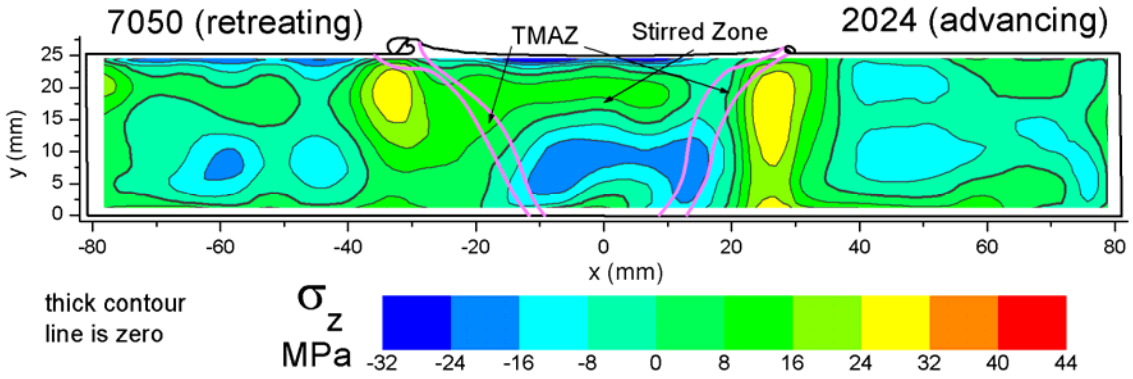

Figure 7. Residual longitudinal stresses measured in test specimen removed from friction stir welded plate. Figure 1 shows the location of the measurement.

Figure 8 shows the neutron diffraction stress results at the measurement points shown in Figure 2. The contour results at the same locations were extracted from the results of Figure 7 and are plotted for comparison.

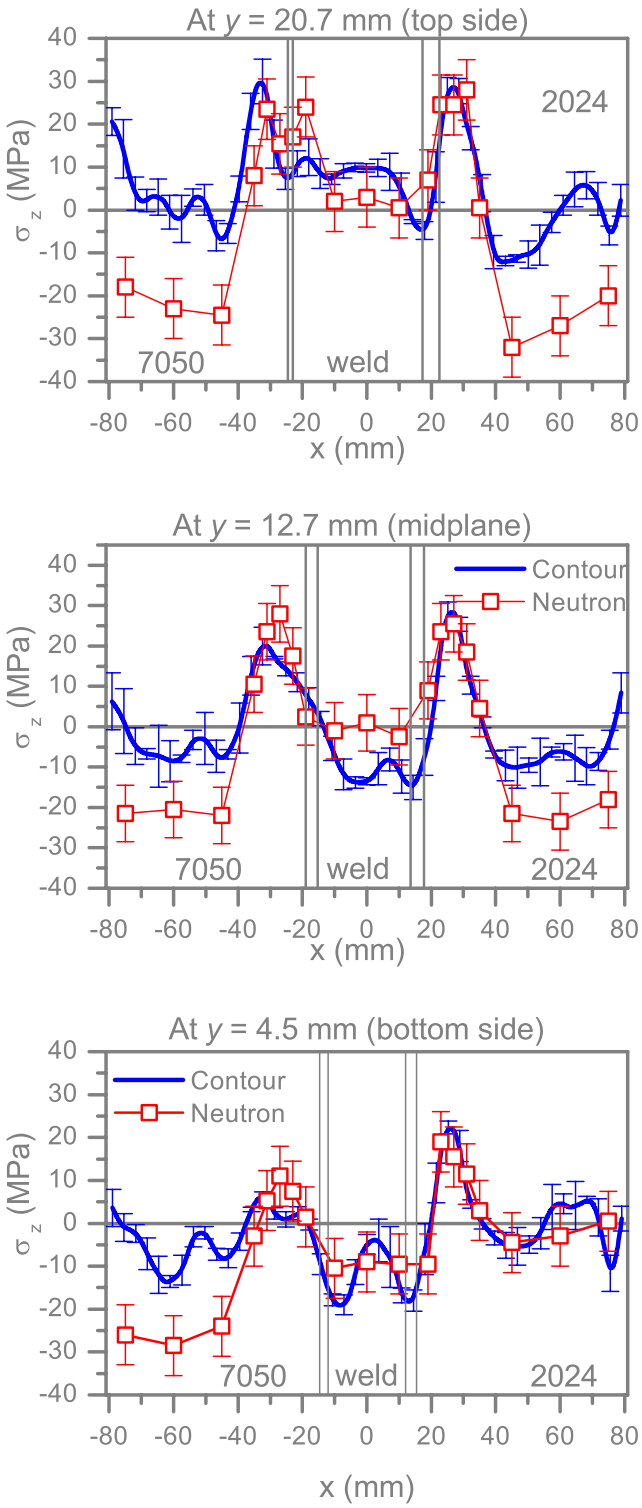

Figure 8. Neutron-diffraction measured stresses plotted with contour results. Vertical lines indicate the stirred zone and TMAZ boundaries.

The test specimen was small enough that removal from the parent plate caused some relaxation of the residual stresses at the measurement locations. An iterative FE procedure was used to estimate the pre-relaxation stresses in the parent plate [33]. In the iterative process, the post-relaxation stresses from Figure 7 were taken as an initial guess for the stresses in the plate prior to removal of the specimen. Using the mesh from Figure 6, the stresses after relaxation were calculated. The difference between the relaxed stresses calculated by the FE model and the measured stresses (Figure 7) was then used to update the guess for the initial stresses in the plate. The iteration converged to within 1 MPa in a few iterations, and Figure 9 shows the result. Comparing with Figure 7, the specimen removal caused the tensile stresses to relax by up to about 10 MPa, or about 25% of the peak value of about 43 MPa.

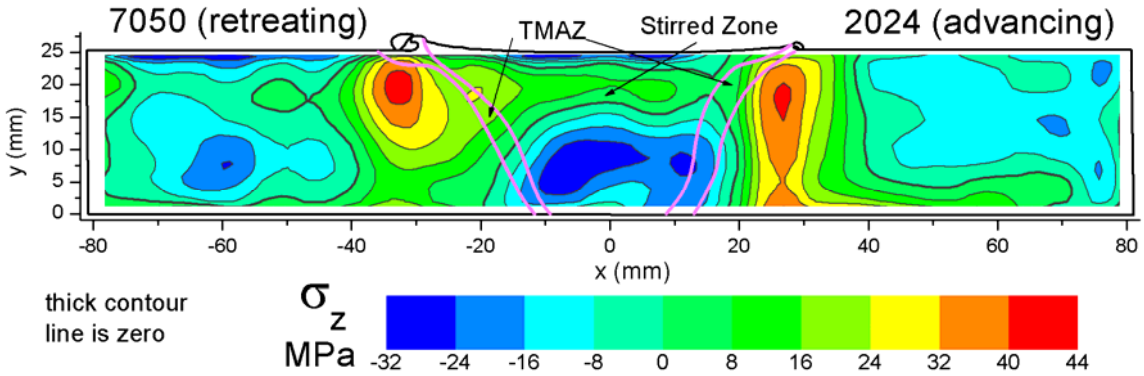

Figure 9. Estimated longitudinal residual stress in parent plate before stresses were partially relaxed from removing test specimen.

IV. Discussion

A. Features in Stress Results

The residual stress distribution follows typical observations for FSW in aluminum alloys in spite of the increased thickness of the specimen examined here relative to previous reports. Tensile residual stresses peak in the heat-affected zone just outside the weld region on both sides giving an “M” shape in Figure 8. The tensile residual stresses occur because of local frictional heating at the tool-material interface. The hotter material

is constrained by other material during cooling, resulting in tensile stresses. The width of the M decreases towards the bottom of the weld, see Figure 8, which corresponds to the shape of the tool which is wider at the top because of the shoulder. A similar observation, measured using synchrotron X-ray diffraction, was reported in 4-mm thick samples [17]. A recent experimental study of pin-only and shoulder-only FSW demonstrated that the frictional heating from the tool shoulder is indeed the main source for the stresses but also that the softening caused by the pin lowers and broadens the lower stress region between the tensile peaks [34]. Outside the weld and heat-affected zone, the background stresses in the base material oscillate between modest magnitudes of tension and compression, consistent with other measurements of pre-FSW residual stresses in the plate after the stress relief by stretching [35, 36].

Some new observations can be made because of the 2D stress map and the relatively thick weld. The peak tensile stresses are closer to the top of the weld, where the tool shoulder is. At the tool shoulder, the relative speeds between the tool and workpiece are the highest, which should lead to the most frictional heating. The peak stresses occur slightly subsurface just as they do in fusion welds because of increasing constraint. Both the contour method and neutron diffraction results show some asymmetry in the stresses. Within measurement uncertainty, the peak tensile stress magnitudes are the same on both sides of the weld. However, the tensile stresses on the advancing side occur through the full thickness of the sample, whereas they are confined to the top half on the retreating side. This asymmetry is consistent with some reports of higher stresses on the advancing side [11, 12, 14]. The heat input on the advancing side should be somewhat higher because of the greater relative velocity between the tool and the workpiece, and this effect was recently shown to come more from the pin than the shoulder [34]. However, the results in this paper are also must have some asymmetry because of the different alloys, and there is insufficient information to sort out the effects. Both the contour method and neutron diffraction results show a compressive stress region that is limited to the bottom half of the plate between the tensile peaks. The observation is consistent with other reports [8, 12, 17, 19] but is resolved much better here in the thick weld and is clearly significant relative to the stresses in the base material. The compressive region is consistent with some aspects of the thermal transients from the welding. The highest

temperatures and temperature gradient regions are first on the top of the weld underneath the tool shoulder and then secondly at the outer surface of the pin. The machining platform underneath the workpiece provides a heat sink and provides cooling preferentially to material near the bottom surface. Thus, the cooler material surrounded by the hotter regions can be pulled into compression by the later cooling and contracting material surrounding it.

The peak residual stress magnitude of 43 MPa Figure 9 is about as low as the best FSW's, indicating an optimized FSW process, but unfortunately is still much too significant to be ignored. In other FSW of aluminum alloys, stresses over 100 MPa have been reported for thinner specimens that are presumably easier to FSW [3, 7, 9, 13, 14, 16]. Therefore, the FSW process for this weld appears to be fairly well optimized at least with regards to residual stresses. For structural metals, residual stresses are usually limited approximately by the yield strength and, thus compared to it. 43 MPa is only 20% of the yield strength of 220 MPa measured in the joint. By comparison, fusion welding generally produces residual stresses well over half of yield and often with individual stress components exceeding yield because of triaxiality [26, 37]. However, as discussed in the Introduction, even the fairly low magnitude stresses of this optimized FSW can have a large effect on fatigue and fracture behavior and on the measurement of fatigue properties [2-6]. A mere 5 MPa residual stress can generate a K_I of greater than 2 MPa·m^{½} in a compact tension specimen, which is the same order as the threshold K_I for fatigue crack growth in these alloys [5].

B. Measurement Issues

The contour and neutron results agree best in the weld region and not as well in the base material. Two possible explanations for the latter are spatial variations of the unstressed lattice spacing d_0 and intergranular stresses. The first hypothesis is supported by Fig. 3(b) which shows notable differences in d_0 from top to bottom of both parent materials caused by inhomogeneous mixing in the weld zone and distance dependent (from the weld) thermal effects in both base materials. The stresses shown in Fig. 8 show that in the base materials the agreement between the neutron method and the contour method is worse near the top surface and best near the bottom surface.

Intergranular stresses can be expected due to the 1.5 % stretching of the parent plates prior to welding. This is reflected by the directional dependence of d_0 shown in Fig. 3(a). The magnitude of the d_0-spread in the x,y, and z-directions, is comparable to results reported for Al7050 [38]. However, a correction using the results from [38] is not possible because of different stretch directions from the work presented here. Ultimately, the effects of d_0-variations from compositional changes and intergranular stresses cannot be separated from each other without sectioning of the specimen and extraction of d_0-coupons from the actual measurement locations. This option was not available.

The excellent agreement between the contour and neutron results in the weld region provides cross-validation of both methods for quite low-magnitude stresses. The peak stresses in the test specimen of about 32 MPa are under 0.05% of the elastic modulus of the material. Previous validations of the contour method have been for stresses over 0.25% of the modulus [26-28]. The uncertainties were estimated at about ±5 MPa for the contour method and ±7 MPa, or 16% and 22% of the stress magnitudes. These uncertainties are quite good for such low stress magnitudes [39]. Also, based on Figure 8, the uncertainty estimates seem to be supported by the comparison between the methods. X-ray studies have shown uncertainties of ±20 MPa to ±100 MPa in aluminum FSW [7], which could have made meaningful measurements difficult in the specimen examined in this paper.

C. Stress Relaxation from Specimen Removal

Contrary to common perception, the test specimen would have had to be quite long in order to avoid significant stress changes such as the 25% reduction in peak stresses estimated for the specimen in this paper. The same simulation used to estimate the relaxation was used to estimate the relaxation for different length specimens [33]. The test specimen would have had to be about 220-mm long in order for the stress at the specimen mid-length to be changed by less than 2%. That is 8.7 times the plate thickness, whereas common perception is that a length of two or three times the specimen thickness is sufficient. St. Venant's principle indicates that the stresses should be largely unchanged one "characteristic distance" away from the cut. In practice for residual stress, this usually amounts to about a 5% change 1.0 characteristic distances away and a 1% change

something like 1.3 distances away (requiring samples 2.0 or 2.6 characteristic distances long to get that change at midlength) [36]. The crucial aspect in applying St. Venant's is determining what makes a characteristic distance. Usually the characteristic distance is assumed to be the thickness, which is valid if the residual stresses vary primarily through the thickness. Examining Figure 7 or Figure 8, the stress distribution varies mostly laterally. The residual stresses mostly equilibrate over the central 90-mm of the cross-section. The 220-mm needed to ensure less than 2% relaxation represents about 2.4 times the 90-mm, which fits within the aforementioned observations on relaxation if 90-mm is taken as the characteristic distance. In general, when the nature of the stress distribution cannot be known *a priori*, it is conservative to take the maximum cross section dimension as the characteristic distance.

V. Conclusions

The measurement by the contour method and neutron diffraction of residual stresses in friction stir weld between 25.4-mm thick plates of 7050-T7451 and 2024-T351 allow several conclusions to be made.

- Even in a FSW of thick, dissimilar, high-strength aluminum alloys, very low residual stresses were achieved. The peak stresses of about 43 MPa are less than 20% of the material yield strength. Such low stresses are virtually unachievable with fusion welding. However, even at those low magnitudes, the residual stresses affect fatigue behavior and the measurement of fatigue properties and, therefore, need to be addressed.
- The contour method and neutron measurement agree within uncertainty limits in the weld region, confirming the ability of both methods to measure fairly low magnitude residual stresses. It is the first validation of the contour method for a stress map peaking at magnitudes below 0.05% of the elastic modulus.
- The measurement differences were probably mostly caused by variations in the unstressed lattice spacing, d_0, together with intergranular stresses in the parent materials, causing errors in the neutron results. This is consistent with other reports, and the issue should be addressed when making diffraction measurements

in FSW specimens. Unfortunately, measuring both d_0 variations and intergranular strains usually requires destroying the specimen.

- For a test specimen removed from a larger piece, the length should be two to three times the characteristic distance in order to maintain the original residual stresses at the specimen mid-length. Unless more information is known, and contrary to common practice, the maximum cross-section dimension should be used as this St. Venant's characteristic distance, not just the thickness.

VI. Acknowledgement

Part of this work was performed at Los Alamos National Laboratory, operated by the University of California for the United States Department of Energy under contract W-7405-ENG-36. Figures 1, 5, 7, and 9 are similar to figures published elsewhere [33] and are reprinted here with the kind permission of the Society for Experimental Mechanics.

Certain commercial firms and trade names are identified in this report in order to specify aspects of the experimental procedure adequately. Such identification is not intended to imply recommendation or endorsement by the National Institute of Standards and Technology, nor is it intended to imply that the materials or equipment identified are necessarily the best available for the purpose.

VII. References

[1] Baumann JA, Lederich RJ, Bolser DR, Talwar R. Property characterization of 2024Al/7075Al bi-alloy friction stir welded joints. In: Jata KM, MW ; Mishra, RS ; Semiatin, SL ; Lienert, T, editor. Friction Stir Welding and Processing II. TMS Publications, 2003. p.199.

[2] Dalle Donna C, Biallas G, Ghidini T, Raimbeaux G. Effect of Weld Imperfections and Residual Stresses on the Fatigue Crack Propagation in Friction Stir Welded Joints. Second International Conference on Friction Stir Welding. Gothenburg, Sweden: The Welding Institute TWI, UK, 2000. p.pdf/CDrom.

[3] Jata KV, Sankaran KK, Ruschau JJ. Friction-stir welding effects on microstructure and fatigue of aluminum alloy 7050-T7451. Metallurgical and Materials Transactions A (Physical Metallurgy and Materials Science) 2000;31A:2181.

[4] Bussu G, Irving PE. The role of residual stress and heat affected zone properties on fatigue crack propagation in friction stir welded 2024-T351 aluminium joints. International Journal of Fatigue 2003;25:77.
[5] John R, Jata KV, Sadananda K. Residual stress effects on near-threshold fatigue crack growth in friction stir welds in aerospace alloys. International Journal of Fatigue 2003;25:939.
[6] Dalle Donna C, Raimbeaux G, Biallas G, Allehaux D, Palm F, Ghidini T. Fatigue Properties of Friction Stir Welded Aluminium Butt Joints ICAF 22, 2003 - Fatigue of Aeronautical Structures as an Engineering Challenge. Lucern, Switzerland, 2003.
[7] James M, Mahoney M, Waldron D. Residual Stress Measurements in Friction Stir Welded Aluminum Alloys. Proc. of the 1st International Symposium on Firction Stir Welding, Rockwell Science Center, California, USA, 1999.
[8] Dalle Donna C, Lima E, Wegner J, Pyzalla A, Buslaps T. Investigations on Residual Stresses in Friction Stir Welds. 3nd International Symposium on Friction Stir Welding, 27 and 28 September 2001. Kobe, Japan: The Welding Institute TWI, UK, 2001. p.pdf/CDrom.
[9] Ya M, Dai F, Lu J. Study of nonuniform in-plane and in-depth residual stress of friction stir welding. Journal of Pressure Vessel Technology 2003;125:201.
[10] Fratini L, Zuccarello B. An analysis of through-thickness residual stresses in aluminium FSW butt joints. International Journal of Machine Tools and Manufacture 2006;46:611.
[11] Peel M, Steuwer A, Preuss M, Withers PJ. Microstructure, mechanical properties and residual stresses as a function of welding speed in aluminium AA5083 friction stir welds. Acta materialia 2003;51:4791.
[12] James MN, Hughes DJ, Hattingh DG, Bradley GR, Mills G, Webster PJ. Synchrotron diffraction measurement of residual stresses in friction stir welded 5383-H321 aluminium butt joints and their modification by fatigue cycling. Fatigue and Fracture of Engineering Material and Structures 2004;27:187.
[13] Webster PJ, Oosterkamp LD, Browne PA, Hughes DJ, Kang WP, Withers PJ, Vaughan GBM. Synchrotron X-ray residual strain scanning of a friction stir weld. Journal of Strain Analysis for Engineering Design 2001;36:61.
[14] Sutton MA, Reynolds AP, Wang DQ, Hubbard CR. A study of residual stresses and microstructure in 2024-T3 aluminum friction stir butt welds. Journal of Engineering Materials and Technology 2002;124:215.
[15] Reynolds AP, Tang W, Gnaupel-Herold T, Prask H. Structure, properties, and residual stress of 304L stainless steel friction stir welds. Scripta Materialia 2003;48:1289.
[16] Wang X-L, Feng Z, David SA, Spooner S, Hubbard CR. Neutron diffraction study of residual stresses in friction stir welds. Proc. of the International Conference on Residual Stresses ICRS 6, vol. 2. Oxford: IOM Communications, London, UK, 2000. p.1408.
[17] Lima EBF, Wegener J, Donne CD, Goerigk G, Wroblewski I, Buslaps T, Pyzalla AR, Reimers W. Dependence of the microstructure, residual stresses and texture of AA 6013 friction stir welds on the welding process. Zeitschrift fur Metallkunde 2003;94:908.
[18] Martins RV, Honkimäki V. A Non-destructive Strain and Phase Investigation of a Friction Stir Weld Joint between an Al-base Metal Matrix Composite and a Monolithic Al Alloy Using Synchrotron Radiation. Journal of Neutron Research;11:277.

[19] Staron P, Kocak M, Williams S. Residual stresses in friction stir welded Al sheets. Applied Physics A: Materials Science and Processing 2002;74:S1161.
[20] Steuwer A, Peel M, Withers PJ, Dickerson T, Shi Q, Shercliff HR. Measurement and Prediction of Residual Stresses in Aluminium Friction Stir Welds. Journal of Neutron Research 2003;11:267.
[21] Prime MB. Cross-sectional mapping of residual stresses by measuring the surface contour after a cut. Journal of Engineering Materials and Technology 2001;123:162.
[22] Prime MB, Newborn MA, Balog JA. Quenching and cold-work residual stresses in aluminum hand forgings: contour method measurement and FEM prediction. Materials science forum 2003;426-432:435.
[23] Martineau RL, Prime MB, Duffey T. Penetration of HSLA-100 steel with tungsten carbide spheres at striking velocities between 0.8 and 2.5 km/s. International Journal of Impact Engineering 2004;30:505.
[24] DeWald AT, Rankin JE, Hill MR, Lee MJ, Chen HL. Assessment of Tensile Residual Stress Mitigation in Alloy 22 Welds Due to Laser Peening. Journal of Engineering Materials and Technology 2004;126:465.
[25] Kelleher J, Prime MB, Buttle D, Mummery PM, Webster PJ, Shackleton J, Withers PJ. The Measurement of Residual Stress in Railway Rails by Diffraction and Other Methods. Journal of Neutron Research 2003;11:187.
[26] Prime MB, Sebring RJ, Edwards JM, Hughes DJ, Webster PJ. Laser surface-contouring and spline data-smoothing for residual stress measurement. Experimental Mechanics 2004;44:176.
[27] Zhang Y, Pratihar S, Fitzpatrick ME, Edwards L. Residual stress mapping in welds using the contour method. Materials science forum 2005;490/491:294.
[28] Zhang Y, Ganguly S, Edwards L, Fitzpatrick ME. Cross-sectional mapping of residual stresses in a VPPA weld using the contour method. Acta materialia 2004;52:5225.
[29] Holt JM, Mindlin H, Ho CY. Structural Alloys Handbook. West Lafayette, IN: CINDAS/Purdue University, 1994.
[30] Allen AJ, Hutchings MT, Windsor CG, Andreani C. Neutron diffraction methods for the study of residual stress fields. Advances in Physics 1985;34:445.
[31] Hauk V. Structural and Residual Stress Analysis by Nondestructive Methods. Amsterdam: Elsevier Science, 1997. p.234ff.
[32] Lienert TJ, Grylls JE, Gould JE, Fraser HL. Deformation Microstructures in Friction Stir Welds on 6061-T651. In: T.R. Bieler LAL, S.R. MacEwen, editor. Hot Deformation of Aluminum Alloys II. 1998 TMS Fall Meeting, Rosemont, Illinois, October 11-15, 1998: TMS, 1998. p.159.
[33] Prime MB, Sebring RJ, Edwards JM, Baumann JA, Lederich RJ. Contour-Method Determination of Parent-Part Residual Stresses Using a Partially Relaxed FSW Test Specimen. 2004 SEM X International Congress & Exposition on Experimental and Applied Mechanics, June 7-10, 2004. Costa Mesa, CA, 2004. p.Paper 144.
[34] Woo W, Choo H, Brown DW, Bourke MAM, Feng Z, David SA, Hubbard CR, Liaw PK. Deconvoluting the influences of heat and plastic deformation on internal strains generated by friction stir processing. Applied Physics Letters 2005;86:231902.
[35] Van Horn KR. Aluminum Vol. III. Fabrication and Finishing. Metals Park, OH: American Society for Metals, 1967.

[36] Prime MB, Hill MR. Residual stress, stress relief, and inhomogeneity in aluminum plate. Scripta Materialia 2002;46:77.
[37] Webster GA, Ezeilo AN. Residual stress distributions and their influence on fatigue lifetimes. International Journal of Fatigue 2001;23:S375.
[38] Pang JWL, Holden TM, Mason TE. In situ generation of intergranular strains in an Al7050 alloy. Acta materialia 1998;46:1503.
[39] Lu J, James M, Roy G. Handbook of Measurement of Residual Stresses. Lilburn, GA: Fairmont Press, 1996.